Journal of Power Sources 287 (2015) 96–99

Contents lists available at ScienceDirect

Journal of Power Sources

journal homepage: www.elsevier.com/locate/jpowsour

Short communication

High performance nickel–palladium nanocatalyst for hydrogen generation from alkaline hydrous hydrazine at room temperature

Debaleena Bhattacharjee, Kaustab Mandal, Subrata Dasgupta*

Ceramic Membrane Division, CSIR-Central Glass & Ceramic Research Institute, 196 Raja S. C. Mullick Road, Kolkata 700 032, India

HIGHLIGHTS

- Ni_xPd_{100-x} nanoalloy catalysts have been synthesized at room temperature.
- Catalytic activities are studied toward hydrazine dehydrogenation.
- $Ni_{60}Pd_{40}$ exhibits the highest catalytic activity at room temperature.
- High selectivity and stability are achieved for H_2 generation from hydrazine.
- NaOH plays an important role as promoter for catalytic dehydrogenation.

GRAPHICAL ABSTRACT

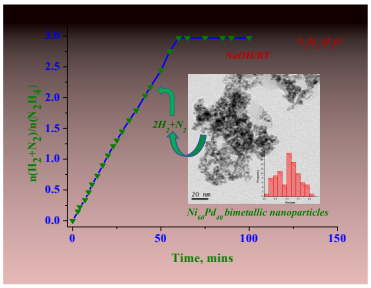

ARTICLE INFO

Article history:
Received 15 December 2014
Received in revised form
11 February 2015
Accepted 3 April 2015
Available online 9 April 2015

Keywords:
Nickel–palladium nanocatalyst
Dehydrogenation
Hydrazine
Catalysis promoter

ABSTRACT

Room temperature synthesized highly active bimetallic $Ni_{60}Pd_{40}$ nanocatalyst with large surface area (150 $m^2\ g^{-1}$) exerts 100% selectivity towards hydrogen generation (3 equivalents of gas in 60 min) from hydrous hydrazine under alkaline and ambient reaction conditions. This low noble metal content catalyst offers a new prospect for on-board hydrogen production system.

1. Introduction

New materials that can facilitate the technological advancements towards transition to a hydrogen economy are of paramount interest. Chemical hydrogen storage materials are of recent interest among material scientists due to their high hydrogen capacities, which is one of the key requirement for developing a hydrogen-based society [1,2]. Lithium and sodium borohydride, ammonia borane and formic acid have been trialled as promising hydrogen storage materials based on their relatively high hydrogen content [3–5]. Recent developments in this direction have suggested hydrous hydrazine ($H_2NNH_2.H_2O$), a liquid over a wide range of temperature (213–392 K) with a hydrogen content as high as 8%, easy recharging as a liquid, is a promising material for hydrogen storage [6–10], since it will only produce nitrogen in addition to hydrogen *via* a complete decomposition reaction $H_2NNH_2 \rightarrow N_2 + 2H_2$ (pathway 1). However, to maximise the usability of hydrazine as a hydrogen storage material, one should avoid the undesired reaction $3H_2NNH_2 \rightarrow 4NH_3 + N_2$ (pathway 2). The reaction

* Corresponding author.
E-mail address: sdasgupta@cgcri.res.in (S. Dasgupta).

http://dx.doi.org/10.1016/j.jpowsour.2015.04.008
0378-7753/

pathways are dependent on the catalyst used and the reaction conditions.

Bimetallic nanoparticles (BMNPs) formed by incorporation of transition metal with noble metal are found to be effective in the field of catalysis due to their unique role of controlling the activity, selectivity and stability as catalysts. The hetero-metallic bond formation with the introduction of a second metal results from the inter-metallic charge transfer or orbital hybridization of the metals. As a consequence of the bimetallic union, the electronic-structural modifications drastically influence the catalytic performance of the mixed-metal catalyst systems showing enhancement in specific properties at an optimum composition because of the synergistic effect of the composition [11–16] and also reduce the use of precious noble metals. Several catalysts like Rh, Ni, Ni–Pd, Rh–Ni, Ni–Pt, Ni–Ir, Ni [7–10,17–19] are presently under investigation for achieving a superior catalytic activity towards hydrogen generation from hydrous hydrazine with 100% selectivity and high catalytic efficiency. Besides synergistic effect, another method to achieve efficiency is the use of high surface area nanoparticles (NPs). In this respect there have grown immense interest for demonstrating ghaphene, carbon nanotubes, activated carbon etc. [19–21] as a promising support material enabling the catalyst to achieve high surface area as a means of increasing the catalytic performance as well as capable of facilitating the electron transfer and mass transport kinetics during the catalytic reaction process.

Here we report a very simple room temperature method of preparing Ni–Pd nanocatalyst (Ni content is 60%) by a surfactant assisted co-reduction of hydroxides of Pd^{2+} and Ni^{2+} by hydrazine without using any support material, still contributing a very high surface area of 150 $m^2\ g^{-1}$, highest reported so far in this class of catalysts, with 100% selectivity towards hydrogen generation from hydrous hydrazine at room temperature where NaOH acts as promoter for complete hydrazine decomposition.

2. Experimental

2.1. Materials

Analytical grade anhydrous $PdCl_2$, nickel chloride, NaOH, hydrazine hydrate and polyvinyl pyrrolidone (PVP) (E. Merck, India) were used without further purification. Mili-Q water was used for the preparation of all solutions.

2.2. Synthesis of Ni_xPd_{100-x} BMNPs

Ni_xPd_{100-x} (x = 50–90) BMNPs were synthesized by co-reduction of hydroxides of Pd^{2+} and Ni^{2+} in presence of PVP at 298 K. 0.0297–0.1191 g of $PdCl_2$ (depending upon the atomic ratio of Pd in Ni_xPd_{100-x}) was dissolved in 20 mL of 0.1 M HCl solution and stirred for 30 min. To that 0.3594–0.2396 g of $NiCl_2$ was added and stirred for another 30 min. The resultant mixture was then added drop wise with constant stirring to 10 mL of 1 M NaOH solution containing 0.0089 g of PVP. Finally, 1 mL of 100% hydrazine hydrate solution was added to it; immediately the black coloured NPs were formed. The NPs were separated, severally washed with deionised water and dried at room temperature. Pd and Ni NPs were synthesized by similar procedure for comparison.

2.3. Structural characterization

The synthesized NPs were characterized using X-ray diffractometer (XRD, Philips 1710, USA) with CuKα radiation (α = 1.541 Å), transmission electron microscopy (TEM, G2 30ST, FEI Company, USA operating at 300 kV), high-resolution TEM (HRTEM), TEM energy dispersion spectroscopy (TEM-EDS) and selected area electron diffraction (SAED) pattern. Adsorption–desorption nitrogen isotherms were obtained using Quantachrome instruments NOVA4000e. Specific surface area (SBET) values were calculated with the Brunauer–Emmett–Teller equation.

A gas chromatograph (YL Instrument 6500GC system, Column: HP-PLOT/Q, HP-Molesieve) connected to a thermal conductivity detector (Valco Instruments Co. Inc.) was used for the analysis of gaseous products.

3. Results and discussions

3.1. Structural characterisation

XRD profiles (Fig. 1) of Pd, Ni and Ni_xPd_{100-x} (x = 50–90) NPs synthesized under similar experimental conditions reveal face centred cubic (fcc) pattern of the prepared nanocatalysts. The XRD pattern of the as prepared Pd and Ni NPs (Fig. 1a and g) exactly matches with the literature reported values (JCPDS, 1995, File no. 05-0681 for Pd and 65-0380 for Ni) indicating the formation of phase pure Pd and Ni NPs only. The Ni_xPd_{100-x} NPs show only one visible prominent diffraction peak corresponding to the (111) plane of palladium. It is observed that with increase in Ni content the diffraction peak of $Ni_{50}Pd_{50}$, $Ni_{60}Pd_{40}$, $Ni_{70}Pd_{30}$, $Ni_{80}Pd_{20}$, $Ni_{90}Pd_{10}$ shift to higher angle compared to that of Pd NPs. The absence of characteristic peak of pure Pd and Ni in the XRD of Ni_xPd_{100-x} NPs (Fig. 1b–f) indicate that the prepared Ni_xPd_{100-x} NPs are composed of bimetallic phase rather than a physical mixture of monometallic Pd and Ni NPs. The XRD pattern of the physical mixture of synthesized Ni and Pd (1:1 mol ratio) is composed of individual peaks corresponding to pure Ni and Pd NPs (ESI, Fig. S1). For the bimetallic phases the XRD peaks appear at 40.50° for $Ni_{50}Pd_{50}$, at 40.60° for $Ni_{60}Pd_{40}$, at 40.62° for $Ni_{70}Pd_{30}$, at 41.10° for $Ni_{80}Pd_{20}$ and at 43.95° for $Ni_{90}Pd_{10}$ NPs. The positions of these XRD peaks clearly show that the diffraction peaks of (111) plane for the synthesized Ni_xPd_{100-x} NPs locate between those of the corresponding planes of the pure Pd (Fig. 1a) and Ni (Fig. 1g) NPs. The shift of the 2θ toward higher angles with increasing the Ni/Pd ratios suggest that the interplanar spacing of the Ni_xPd_{100-x} BMNPs changes with the composition of the feed molar ratio of Ni to Pd. As expected, the trend that the lattice parameters follow (ESI, Table S1) is indicative of alloy formation where the lattice contraction occurred with an increase in nickel content due to the substitution of smaller nickel atoms for larger palladium atoms [22–24]. The Ni_xPd_{100-x} bimetallic structure can be explained by Hume–Rothery rule [25,26], which states that when the relative differences of the atomic radii

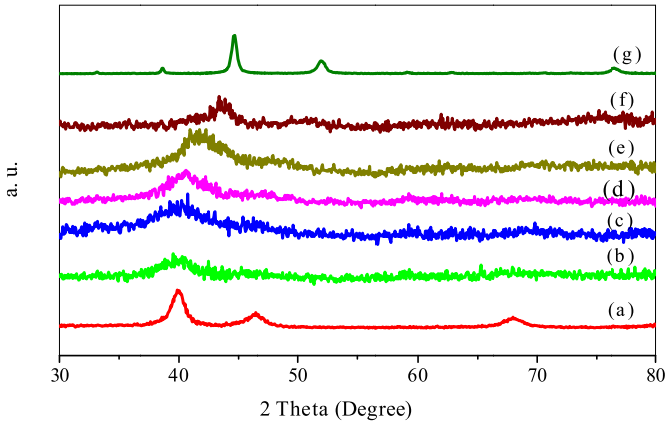

Fig. 1. XRD patterns of the (a) Pd, (b) $Ni_{50}Pd_{50}$, (c) $Ni_{60}Pd_{40}$, (d) $Ni_{70}Pd_{30}$, (e) $Ni_{80}Pd_{20}$, (f) $Ni_{90}Pd_{10}$ and (g) Ni NPs.